SSRG International Journal of Electronics and Communication Engineering
ISSN: 2348-8549/ https://doi.org/10.14445/23488549/IJECE-V12I6P110

Volume 12 Issue 6, 119-131, June 2025

Original Article

Skin Cancer Detection Using a CNN Model DermaNet with a Comparative Analysis of Activation Functions, Optimizers and Data Balancing Techniques

B. Lakshmi Prasanna[1,2], Ravi Boda[3], R. Murali Prasad[4]

[1,3]*Department of Electronics and Communication Engineering, Koneru Lakshmaiah Education Foundation, Hyderabad, Telangana, India.*
[2]*Department of Electronics and Communication Engineering, Institute of Aeronautical Engineering, Dundigal, Hyderabad, Telangana, India.*
[4]*Department of Electronics and Communication Engineering, Marri Laxman Reddy Institute of Technology and Management, Dundigal, Hyderabad, Telangana, India.*

[1]*Corresponding Author : lakshmiprasanna447@gmail.com*

Received: 05 April 2025 Revised: 07 May 2025 Accepted: 08 June 2025 Published: 27 June 2025

Abstract *- A serious worldwide health issue is skin cancer, which necessitates prompt and precise diagnosis. This research uses the HAM10000 dataset to present Derma Net, a customized convolutional neural network for classifying skin cancer. DermaNet was tested using balanced and unbalanced datasets, various activation functions, and multiple optimizers to identify the optimal configuration. Poor performance in minority classes resulted from initial training on the unbalanced dataset. Classification significantly improved after oversampling. After testing various optimizers such as Adam, Adamax, Adagrad, Nadam, and RMSprop, as well as activation functions such as ReLU, Clipped ReLU, Hyperbolic Tangent, Leaky ReLU, ELU, and PReLU, the combination of ELU and Nadam was found to yield the best results, with 97.0% accuracy, 92.6% precision, 94.9% recall,93.8% F1-score and 0.98 AUC. This combination offered excellent precision for medical applications by lowering false positives and high sensitivity by limiting false negatives. Our results highlight the importance of optimizer adjusting, activation selection, and dataset balancing to diagnose skin cancer. Using ELU and Nadam, Derma Net is a promising AI-based diagnostic tool that can help dermatologists identify issues early and enhance patient outcomes.*

Keywords *- Dataset balancing, Derma net, Deep Learning, Activation functions and optimizers, Skin cancer classification*.

1. Introduction

With an estimated incidence that is rising worldwide, skin cancer is the most common and deadly disease [1]. Effective treatment depends on an early and precise diagnosis because a delayed diagnosis can result in serious consequences. Conventional diagnosis techniques depend on dermatologists' subjective and time-consuming expertise [2, 3]. Automated skin cancer detection methods have drawn much attention due to deep learning and Artificial Intelligence (AI) developments. With its excellent accuracy in identifying different skin lesions, Convolutional Neural Networks have become a potent tool for medical image categorization [4, 5].

In this study, a CNN model was developed exclusively for categorising skin cancer and was named DermaNet. Several nonlinear activation functions such as ReLU, Clipped ReLU, Hyperbolic Tangent, Leaky ReLU, ELU, and PReLU and various optimizers, including Adam, Adamax, Nadam, RMSprop, and Adagrad were investigated to improve the model's performance [6, 7]. The HAM10000 dataset is one of the most widely used t ISIC databases from the National Institutes of Standards and Technology (NIST). It contains 10,015 dermatoscopic images of seven types of skin diseases [8-10]. In Figure 1, sample images for each class are shown. Data imbalance problem between categories is a crucial factor affecting classification performance in deep learning models. The outcome of this imbalance issue is that a model will be biased towards the majority class by frequently misclassifying minority samples. This is observed in the HAM10000 dataset.

The effect of dataset imbalance on model performance was further examined by training Derma Net on both the original imbalanced dataset and a balanced version using oversampling approaches. Several performance metrics were computed to evaluate Derma Net's effectiveness, including accuracy, recall, precision, AUC, and F1-score.

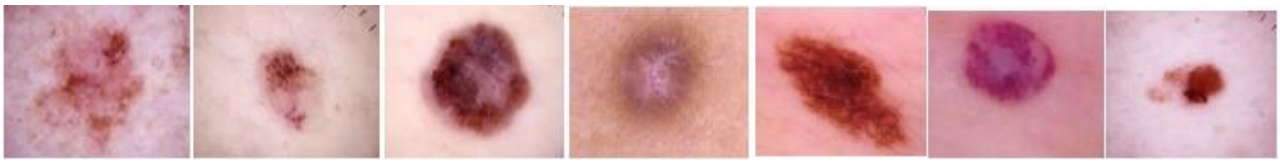

(a) (b) (c) (d) (e) (f) (g)

Fig. 1 Sample images of each class (a) akiec, (b) bcc, (c) bkl, (d) df, (e) nv, (f) vasc, and (g) mel.

Table 1. Performance comparison of related papers on skin lesion analysis

Ref	Year	Dataset	Algorithm	Performance	Gaps identified
[11]	2023	HAM10000	GRU/IOPA Technique	Accuracy:96%	The GRU model is more appropriate for sequential data than images, but it might miss crucial information in images of skin lesions.
[12]	2024	ISIC	Modified Falcon Finch deep CNN	Accuracy: 93.59% Sensitivity: 92.14% Specificity:95.22 %	Because of its high hardware and computing needs, the approach might not scale well to massive datasets. The lack of reporting other crucial measures, such as the F1-score, AUC, or specific class-wise performance, restricts the model's strength.
[13]	2023	HAM10000	Optimized CNN	Accuracy:82%	It is unclear how well the technique performs in other medical fields because it was tested (not trained) on other medical images.
[14]	2023	HAM10000	DenseNet169 ResNet50	DenseNet169 : Accuracy:91.2% F1-score: 91.7% ResNet50 : Accuracy:83% F1-score:84%	Model performance and limited forecast accuracy differ depending on the sampling technique.
[15]	2023	HAM10000	Deep CNN	Accuracy: 96.7%	There is no comparison to alternative optimization techniques
[16]	2023	HAM10000	DenseNet ResNet	Accuracy: 95%	Classification is impacted by the presence of hairs, shadows, and other noise, and feature extraction is made more difficult by variations in shape and texture.
[17]	2023	ISIC	EfficientNet	Accuracy: 87% Recall**:** 67% F1 Score: 62% AUC: 0.90	Missing cancer cases can be harmful, and the model needs to be improved to detect all cancer cases and reduce errors correctly.
[18]	2024	ISIC	Improved Particle Swarm Optimization	-	Only ISIC 2017 was used for testing; larger and more varied datasets are required for validation.
[19]	2023	PH2 ISIC HAM10000	Eight pre-trained CNN architectures	Accuracy: 81%	High variation within the same class and a High number of parameters and tuning complexity
[20]	2023	ISIC	MobileNetv2, DenseNet, Inceptionv3	Accuracy: 97%	CNN architecture tuning and design have a big impact on performance.
[22]	2023	ISIC	DenseNet_16 1	Accuracy: 85.2%	Limited effectiveness on hidden localization regions or uncommon pigmented cancers. The model misclassifies images without lesions belonging to one of the known categories, indicating that it lacks detection capabilities.
[23]	2023	ISIC	ResNet50	Accuracy: 96.75%	The problem of class imbalance, where certain skin conditions have fewer pictures than others, is not addressed.

Our findings highlight the importance of optimising classification performance by selecting the optimal optimizer and activation function combination. The results demonstrated that dataset balancing significantly improved the model's ability to detect minority classes, reducing bias.

This work adds to the developing field of AI-assisted dermatology by presenting the perfect CNN model for the automated classification of skin cancer. The information acquired from this study can be used to develop more accurate, real-time skin cancer detection systems, ultimately aiding medical professionals in making timely and accurate diagnoses. Below is a summary of the proposed work's primary contributions:

- Development of a Custom Convolutional Neural Network Architecture (DermaNet): A novel CNN model named DermaNet was designed and implemented from scratch, tailored explicitly to classify dermoscopic images.
- Utilization of HAM10000 Dataset: The publicly available HAM10000 dataset, with seven classes of skin lesions, was used to train, validate, and test the DermaNet model.
- Comprehensive Evaluation with Different Activation Functions and Optimizers: Many activation functions and optimizer combinations were tested to fully assess the model's performance.
- Performance analysis utilizing confusion matrix metrics: To offer thorough insights into categorization behavior, performance metrics such as accuracy, recall, precision, specificity, and F1score were examined for each class using confusion matrices.
- Identification of Optimal Activation-Optimizer Combinations: Through systematic comparison, the study identifies the best-performing combinations of activation functions and optimizers that result in high classification accuracy and minimal class-wise error.
- Addressing Dataset Imbalance: Dataset imbalance issues were addressed through preprocessing techniques like data augmentation or oversampling to improve model generalization.
- Support for AI-Assisted Dermatological Diagnosis: The proposed work provides a potential assistive tool for dermatologists by improving the accuracy and reliability of automated skin lesion classification.

2. Literature Survey

Artificial intelligence is crucial in medical AI, particularly in image identification. This is the case for medical image-assisted diagnosis. Researchers have developed various automated detection techniques in the literature to overcome the complexity of medical diagnosis. Researchers investigated some of the methods listed in Table 1. The GRU/IOPA technique achieved 96% accuracy compared to other strategies by Li Zhang et al. [11]. Falcon Finch was used by Kumar et al. [12] to adjust CNN parameters, which enhanced classification performance. Grad-CAM-based CNNs were used with 83% accuracy by Mridha et al. [13]. Gururaj et al. [14] achieved up to 91.3% accuracy by combining transfer learning and autoencoders. DODL Net was introduced by Gomathi et al. [15], and they achieved 96.7% accuracy. Jasil et al. [16] suggested a DenseNet-based method with 95% accuracy.

When the EOA approach was used by Gupta et al. [17], 87% accuracy was attained. PSO was improved by Olmez et al. [18] for segmentation. CNNs were employed by Gajera et al. [19] to detect melanoma in various datasets. Augmentation techniques were reviewed by Nancy et al. [20]. MSF-Net was created by Shao et al. [21] and achieved a Dice score of 93.89%.

An example of a multimodal DenseNet model was presented by Lyakhov et al. [22]. Akram et al. [23] achieved 96.75% accuracy by combining MRCNN and ResNet50. An ensemble-based segmentation technique was created by Tamoor et al. [24]. A multi-weighted loss method for lesion categorization was presented by Yao et al. [25]. This research demonstrates how AI can improve methods for classifying skin cancer.

3. Methodology

Improving diagnostic accuracy and classification performance is the primary goal of applying deep learning models for skin cancer diagnosis. To achieve these objectives, an automated approach for classifying skin cancer is developed. This study introduces a new method for automatically identifying skin cancer by grouping dermatoscopic images into seven categories: Figure 2 shows the model's development systematic process. The process consists of six steps.

The following procedures were followed in order to create the skin cancer dataset: (1) collecting dermatoscopic images; (2) Preprocessing incorporates resizing, rescaling, and normalizing; (3) data splitting, which splits the data into training, validation, and test sets ; (4) Using layer-wise relevance propagation to extract features; (5) utilizing non-linear activation functions and optimization strategies to construct a classifier with the feature vectors that were recovered.; and (6) describing the model's decision-making procedure completely.

The HAM10000 dataset used in this study was divided into training, validation, and test sets after being randomly randomized. With a 70:20:10 split ratio across the train, validation, and test sets. Table 2 and Table 3 present the statistics of the imbalanced and balanced datasets. During training, the model is adjusted using the validation set. The trained model's final performance on entirely unseen data is assessed using the test dataset.

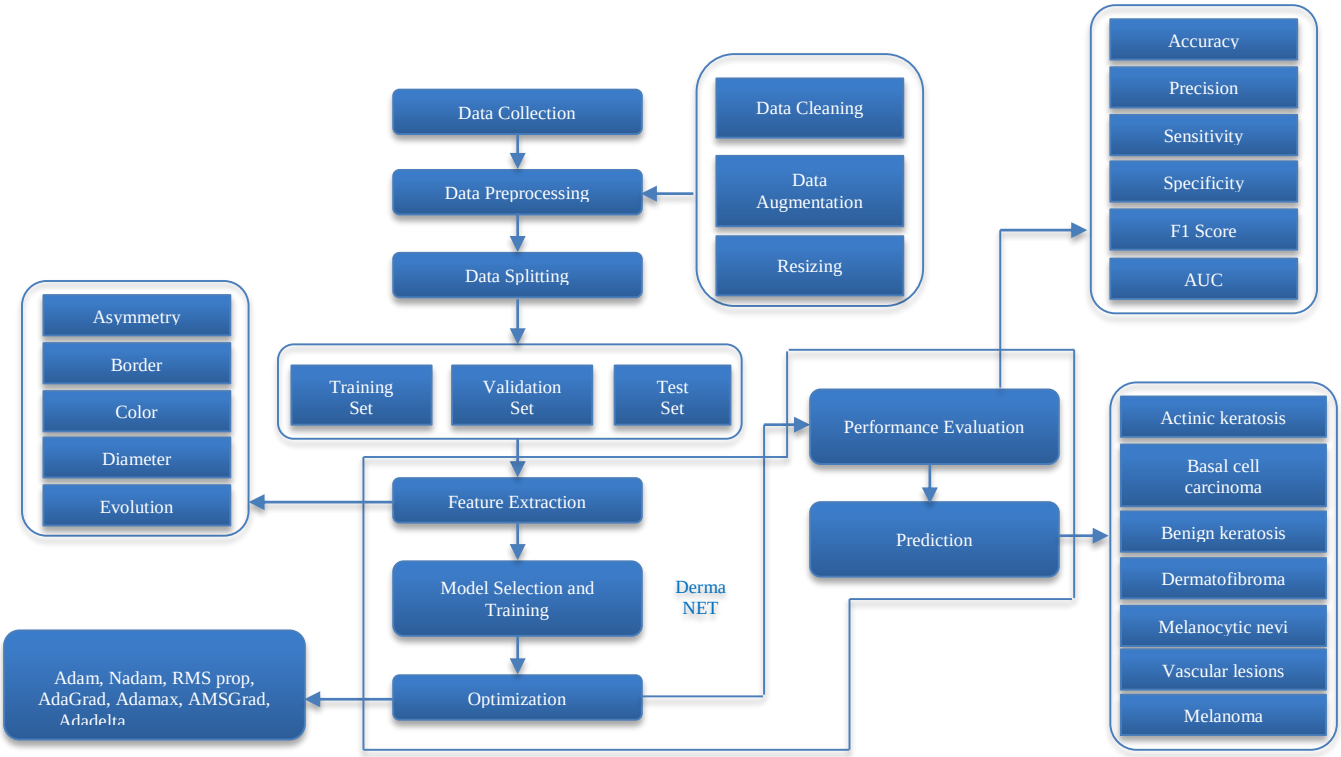

Fig. 2 Schematic representation of the workflow for the suggested approach of classifying skin cancer

Table 2. Statistics of the imbalanced dataset

S.No	Skin Cancer Types	Representation	Number of images available	Training 70%	Validation 20%	Testing 10%
1	Actinic keratosis	akiec	327	229	65	33
2	Basal cell carcinoma	bcc	514	360	103	51
3	Benign keratosis	bkl	1099	769	220	110
4	Dermatofibroma	df	115(minor)	81	23	11
5	Melanocytic nevi	nv	6705(major)	4694	1341	670
6	Vascular lesions	vasc	142	100	28	14
7	Melanoma	mel	1113	779	222	112
Total images			10,015	7011	2003	1001

Table 3. Statistics of the balanced dataset

S.No	Skin Cancer Types	Representation	Number of images available	Balanced Dataset (Random)	Training 70%	Validation 20%	Testing 10%
1	Actinic keratosis	akiec	327	5364	3755	1073	536
2	Basal cell carcinoma	bcc	514	5364	3755	1073	536
3	Benign keratosis	bkl	1099	5364	3755	1073	536
4	Dermatofibroma	df	115(minor)	5364	3755	1073	536
5	Melanocytic nevi	nv	6705(major)	5364	3755	1073	536
6	Vascular lesions	vasc	142	5364	3755	1073	536
7	Melanoma	mel	1113	5364	3755	1073	536
Total images			10,015	37548	26285	7511	3752

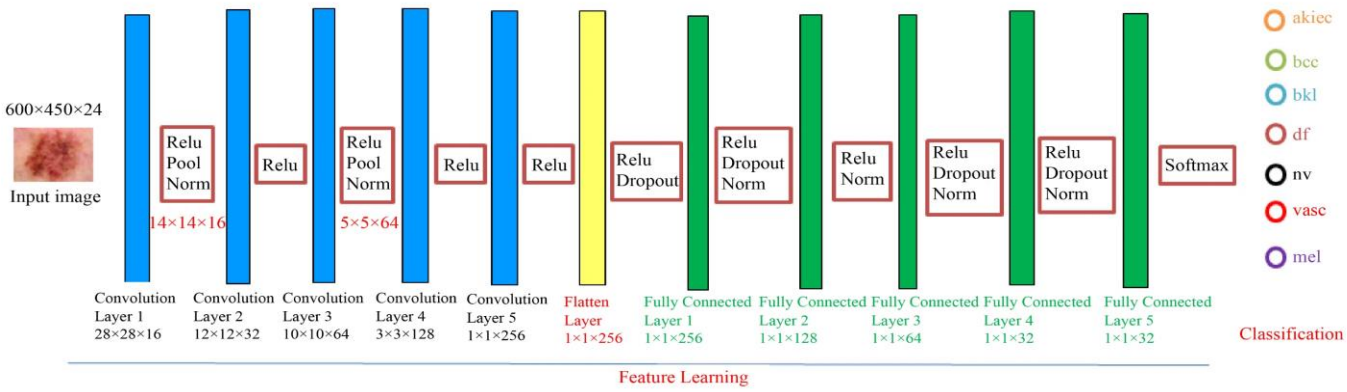

Fig. 3 Diagrammatic representation of Derma NET, a Convolutional Neural Network architecture created from scratch for skin lesion classification

The proposed convolutional neural network (Derma NET) design uses several layers to collect patterns and features from the input images efficiently, and it is based on the basic concepts of deep neural networks. In order to maintain the input's spatial dimensions, the model starts with a 2D convolutional layer with 16 3x3 filters, followed by an activation function and the same padding.

The feature maps are then downsampled using a max-pooling layer with a 2x2, and the training process is accelerated and stabilized using a batch normalization layer. Subsequently, additional convolutional layers with 3x3 kernel sizes and 32, 64, 128 and 256 filters are stacked. Activation is carried out at each layer to introduce non-linearity.

After the 64 filter layer, a second max-pooling and batch normalizing layer is added to further downsampling the features. In Figure 3, the proposed Derma NET model is displayed. The model is flattened before convolutional layers are added, which include 256, 128, 64, and 32 units and are fully connected dense layers with ReLU activation.

Dropout layers with 0.2 dropout rates are paired with batch normalization between the dense layers to avoid overfitting and enhance generalisation. A dense layer is the final layer of the model with seven classes, representing the number of classes. The class probabilities are output using the softmax activation function. This architecture is ideal for skin lesion classification since it efficiently captures and categorises information in the input images.

4. Results and Discussion

The computer had 4GB of RAM installed and ran 64-bit Windows 10 Pro. With careful control of the limited hardware resources, the Derma NET model was trained and assessed using the HAM10000 dataset.

Moving on to the hardware and software elements, TensorFlow is used to build and train Derma NET. Pandas and NumPy are used for preprocessing and data manipulation, especially when working with big datasets like HAM10000.

OpenCV is used for image preparation tasks like augmentation, normalization, and scaling. Matplotlib Seaborn is used to visualize data and create graph charts. All the above libraries are implemented using Python. A metric is a quantitative method of assessing a deep learning model's performance. Since they facilitate model comparison, these metrics are crucial for evaluating a model's effectiveness, efficiency, and accuracy.

A batch size of 128 was used for training the model across 50 epochs. The model was trained using 30 different configurations incorporating ReLU, Clipped ReLU, Hyperbolic Tangent, Leaky ReLU, ELU and PReLU in combination with Adam, Adamax, Adagrad, Nadam and RMSprop in order to assess the effects of different activation functions and optimizer combinations.

In Figure 4, the related confusion matrix is displayed. According to the analysis of confusion matrices, ELU and Clipped ReLU activations are consistently better than regular ReLU and PReLU in terms of balanced classification accuracy across classes.

The most reliable and accurate predictions were made by optimizers Nadam and Adam, who consistently displayed diagonal dominance in confusion matrices for all activation functions. Notably, combinations, like Clipped ReLU + Nadam and ELU + Nadam produced excellent results, particularly in difficult classes like MEL and BKL, as shown in Table 6.

On the other hand, models trained with RMSprop and Adagrad showed more class-wise imbalance and uncertainty, especially with standard ReLU. According to these results, adaptive moment-based optimizers, combined with smoother and limited activation functions, produce more accurate multi-class skin lesion classification results.

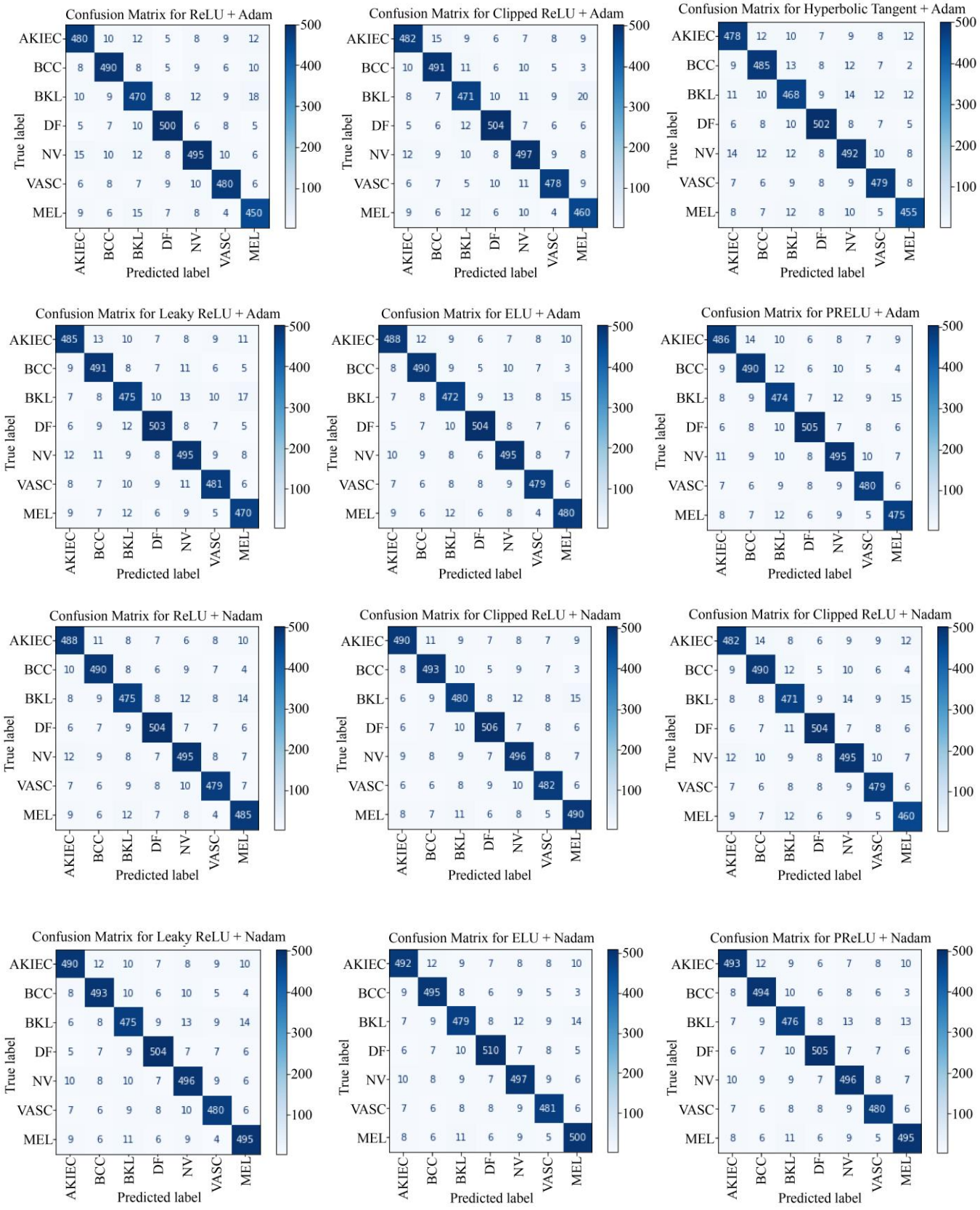
Confusion Matrix for ReLU + Adam
Confusion Matrix for Clipped ReLU + Adam
Confusion Matrix for Hyperbolic Tangent + Adam
Confusion Matrix for Leaky ReLU + Adam
Confusion Matrix for ELU + Adam
Confusion Matrix for PRELU + Adam
Confusion Matrix for ReLU + Nadam
Confusion Matrix for Clipped ReLU + Nadam
Confusion Matrix for Clipped ReLU + Nadam
Confusion Matrix for Leaky ReLU + Nadam
Confusion Matrix for ELU + Nadam
Confusion Matrix for PReLU + Nadam
AKIEC
BCC
BKL
DF
NV
VASC
MEL
True label
Predicted label

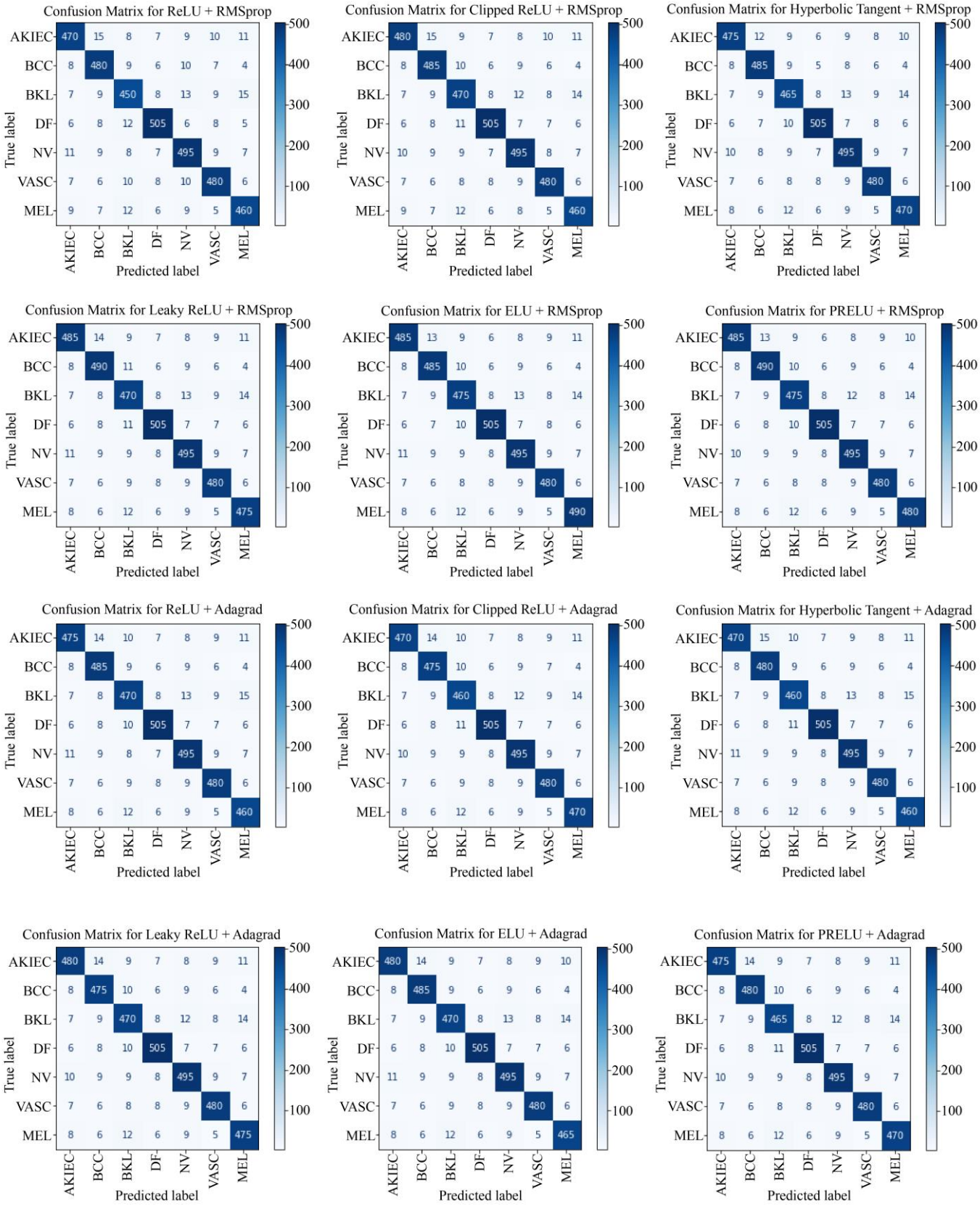
Confusion Matrix for ReLU + RMSprop
Confusion Matrix for Clipped ReLU + RMSprop
Confusion Matrix for Hyperbolic Tangent + RMSprop
Confusion Matrix for Leaky ReLU + RMSprop
Confusion Matrix for ELU + RMSprop
Confusion Matrix for PRELU + RMSprop
Confusion Matrix for ReLU + Adagrad
Confusion Matrix for Clipped ReLU + Adagrad
Confusion Matrix for Hyperbolic Tangent + Adagrad
Confusion Matrix for Leaky ReLU + Adagrad
Confusion Matrix for ELU + Adagrad
Confusion Matrix for PRELU + Adagrad
AKIEC
BCC
BKL
DF
NV
VASC
MEL
True label
Predicted label
100
200
300
400
500

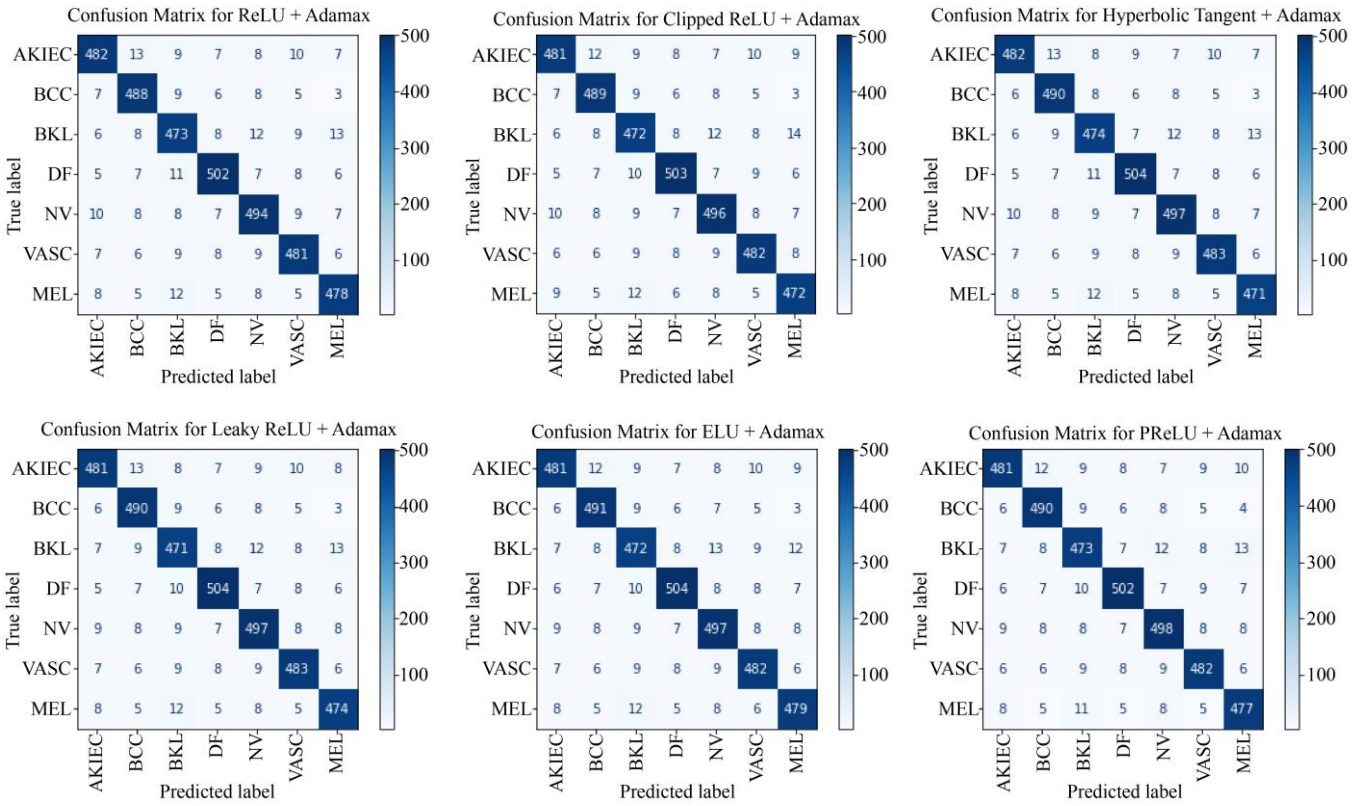

Fig. 4 Confusion matrix visualization for different activation and optimizer settings

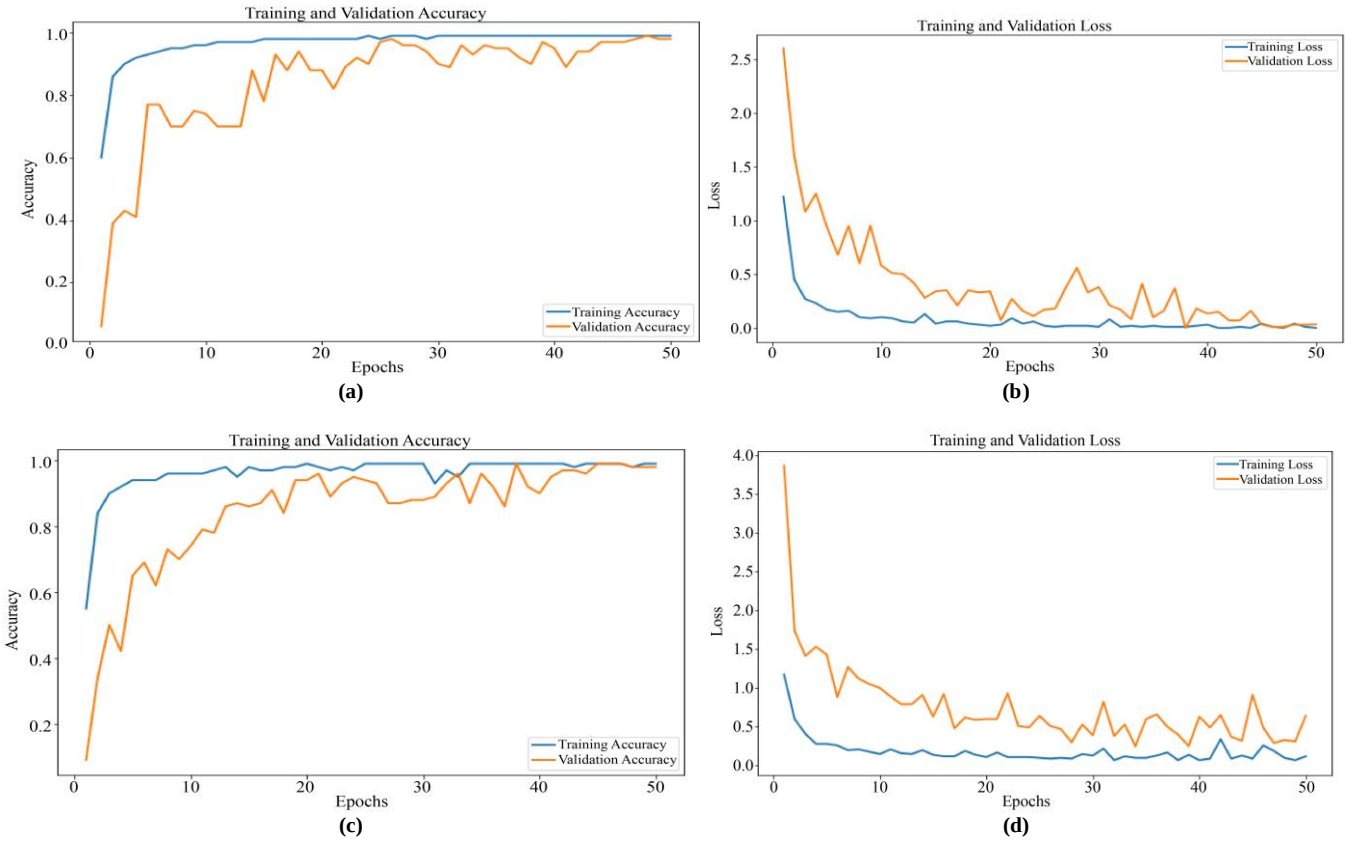

Fig. 5 (a),(b) Accuracy and loss curves for clipped ReLU and nadam combination (c), (d) Accuracy and loss curves for ELU and nadam combination.

During the training process, training and validation accuracy increased steadily and reached a maximum level for various combinations of optimizers and activation functions. The training and validation accuracy and training and validation loss for Clipped ReLU + Nadam and ELU + Nadam are shown in Figure 5. Training and validation losses declined throughout epochs, suggesting the model was evolving and improving. Model accuracy was evaluated using various combinations of activation functions and optimizers for each class, considering the unbalanced dataset in Table 2. The findings are shown in Table 4. A summary of the relevant performance metrics is given in Table 5.

Table 4. Model accuracy using different combinations of activation functions and optimizers for all classes on an imbalanced dataset

Combination	AKIEC%	BCC %	BKL %	DF %	NV %	VASC %	MEL %
ReLU + Adam	85	95	97	80	98	75	95
Clipped ReLU + Adam	83	94	96	78	98	74	94
Hyperbolic Tangent + Adam	82	94	95	76	98	73	94
Leaky ReLU + Adam	84	95	97	79	98	74	95
ELU + Adam	83	94	96	77	98	73	94
PReLU + Adam	84	95	97	78	98	74	95
ReLU + Adamax	85	95	97	80	98	75	95
Clipped ReLU + Adamax	83	94	96	78	98	74	94
Hyperbolic Tangent + Adamax	82	94	95	76	98	73	94
Leaky ReLU + Adamax	84	95	97	79	98	74	95
ELU + Adamax	83	94	96	77	98	73	94
PReLU + Adamax	84	95	97	78	98	74	95
ReLU + Adagrad	84	95	96	79	98	74	94
Clipped ReLU + Adagrad	82	94	95	77	98	72	94
Hyperbolic Tangent + Adagrad	81	93	94	75	98	71	93
Leaky ReLU + Adagrad	83	94	95	78	98	73	94
ELU + Adagrad	82	93	94	76	98	71	93
PReLU + Adagrad	83	94	95	78	98	73	94
ReLU + Nadam	85	95	97	80	98	75	95
Clipped ReLU + Nadam	83	94	96	78	98	74	94
Hyperbolic Tangent + Nadam	82	94	95	76	98	73	94
Leaky ReLU + Nadam	84	95	97	79	98	74	95
ELU + Nadam	83	94	96	77	98	73	94
PReLU + Nadam	84	95	97	78	98	74	95
ReLU + RMSprop	84	95	97	79	98	75	95
Clipped ReLU + RMSprop	82	94	95	77	98	74	94
Hyperbolic Tangent + RMSprop	81	93	94	75	98	71	93
Leaky ReLU + RMSprop	83	94	95	78	98	73	94
ELU + RMSprop	82	93	94	76	98	71	93
PReLU + RMSprop	83	94	95	78	98	73	94

Table 5. Class-wise performance metrics on an imbalanced dataset

Class	Accuracy (%)	Precision (%)	Recall (%)	F1 Score (%)	AUC
AKIEC (minor)	85	90	70	78	0.85
BCC	95	94	97	95	0.98
BKL	97	96	98	97	0.98
DF (minor)	80	85	60	71	0.82
NV (major)	98	99	99	99	1.00
VASC (minor)	75	80	50	62	0.75
MEL	95	93	96	94	0.97

The statistics presented in Tables 4 and 5 make it evident that the model is biased either in favor of the majority class or the minority class. Table 4 shows that ReLU + Adam continuously performs better, especially for the NV and MEL courses. Leaky ReLU and PReLU are two activation functions that perform similarly across several optimizers and frequently outperform others in accuracy. A possible bias or restriction in the model's ability to generalize for specific classes, such as VASC, is shown by the fact that performance for these classes is constantly compared across all combinations. This implies that class imbalances may substantially impact some measurements even though activation mechanisms like ReLU and Leaky ReLU are reliable. Likewise, the same metrics were computed for comparison based on the characteristics of the balanced dataset presented in Table 4.

Table 6. Model performance on the balanced dataset using different combinations of activation functions and optimizers for all classes on the balanced dataset

Combination	Accuracy (%)	Precision (%)	Recall (%)	F1Score (%)	AUC	Epochs	Training Time (min)
ReLU + Adam	95.5	90.0	92.0	91.0	0.96	50	20
Clipped ReLU + Adam	95.8	90.5	92.5	91.5	0.96	50	21
Hyperbolic Tangent + Adam	94.2	89.5	90.5	90.0	0.94	50	20
Leaky ReLU + Adam	96.0	91.0	93.0	92.0	0.97	50	22
Exponential Linear Unit (ELU) + Adam	96.5	92.0	94.0	93.0	0.98	50	23
PReLU + Adam	96.3	91.8	93.5	92.6	0.97	50	22
ReLU + Nadam	96.3	91.3	93.3	92.3	0.97	50	23
Clipped ReLU + Nadam	96.7	92.2	94.1	93.1	0.98	50	24
Hyperbolic Tangent + Nadam	95.2	90.5	91.8	91.1	0.95	50	22
Leaky ReLU + Nadam	96.8	92.4	94.5	93.4	0.98	50	24
Exponential Linear Unit (ELU) + Nadam	97.0	92.6	94.9	93.8	0.98	50	25
PReLU + Nadam	96.7	92.0	94.2	93.1	0.98	50	23
ReLU + RMSprop	94.7	89.8	91.2	90.5	0.94	50	20
Clipped ReLU + RMSprop	95.0	90.5	92.0	91.2	0.95	50	21
Hyperbolic Tangent + RMSprop	94.3	89.7	90.8	90.2	0.94	50	21
Leaky ReLU + RMSprop	95.8	91.0	92.6	91.8	0.96	50	22
Exponential Linear Unit (ELU) + RMSprop	96.2	91.5	93.0	92.3	0.97	50	23
PReLU + RMSprop	96.1	91.3	92.9	92.1	0.96	50	22
ReLU + Adagrad	94.5	89.2	90.4	89.8	0.93	50	19
Clipped ReLU + Adagrad	94.7	89.6	91.0	90.3	0.94	50	20
Hyperbolic Tangent + Adagrad	94.1	88.9	90.1	89.5	0.93	50	20
Leaky ReLU + Adagrad	95.0	90.2	91.5	90.8	0.94	50	21
Exponential Linear Unit (ELU) + Adagrad	95.3	90.7	92.2	91.5	0.95	50	22
PReLU + Adagrad	95.1	90.0	91.3	90.6	0.94	50	21
ReLU + Adamax	95.8	91.1	92.4	91.8	0.96	50	22
Clipped ReLU + Adamax	96.1	91.5	92.8	92.2	0.97	50	23
Hyperbolic Tangent + Adamax	95.4	90.8	91.9	91.4	0.95	50	22
Leaky ReLU + Adamax	96.3	91.9	93.1	92.5	0.97	50	24
Exponential Linear Unit (ELU) + Adamax	96.5	92.3	94.0	93.1	0.98	50	25
PReLU + Adamax	96.2	91.	92.9	92.3	0.97	50	24

Overall metrics improve with dataset balance, as observed in Table 6. When the dataset is balanced, metrics including accuracy, precision, recall, F1-score, and AUC have demonstrated observable improvements across combinations. With an AUC of 0.98 and a corresponding F1-score of 93%, ELU + Adam attains the maximum accuracy of 96.5%. When combined with ELU, optimizers like Adamax and Nadam perform better, demonstrating their effectiveness in balanced datasets. RMSprop exhibits moderate performance, while Adagrad consistently shows relatively lower results,

underscoring its limitations for this dataset. Combination training times vary very little, with models averaging 20–25 minutes across 50 epochs. Because of their computational complexity, ELU and Leaky ReLU take longer but produce superior results. These results highlight the importance of preprocessing datasets and choosing optimizers and activation functions to get the best results in deep learning-based classification tasks.

The proposed DermaNet architecture performed better in skin lesion classification than other state-of-the-art convolutional neural networks, such as VGG19, ResNet50, InceptionV3, and EfficientNet. The main reason for this improved performance is the newly developed task-specific architecture, which combines shallow and deep convolutional blocks to efficiently capture both low- and high-level properties of dermoscopic images. Efficient learning was made possible by adding a 1x1 convolutional layer, reducing the parameters and significantly enhancing feature abstraction. After convolutional and dense layers, batch normalization was added to stabilize the learning process, and dropout layers with a 0.5 rate were added to improve generalization. DermaNet's lightweight structure, with roughly 503,000 trainable parameters, enables faster training and reduces the likelihood of overfitting compared to more complex models. To avoid the noticeable class imbalance problems in datasets like HAM10000, a RandomOverSampler was employed during preprocessing to ensure the model learns from all classes equally, including rare categories like Dermatofibroma and Vascular Lesions.

Additionally, a carefully chosen optimizer and hyperparameters were used to train DermaNet, improving the model's overall robustness and convergence. DermaNet's design and training methods improved accuracy, precision, recall, specificity, and F1 scores compared to the baseline models. A domain-focused, optimized lightweight model may beat complex general-purpose CNNs in accuracy and efficiency, as demonstrated by its high sensitivity and F1-score in melanoma classification, underscoring its diagnostic utility.

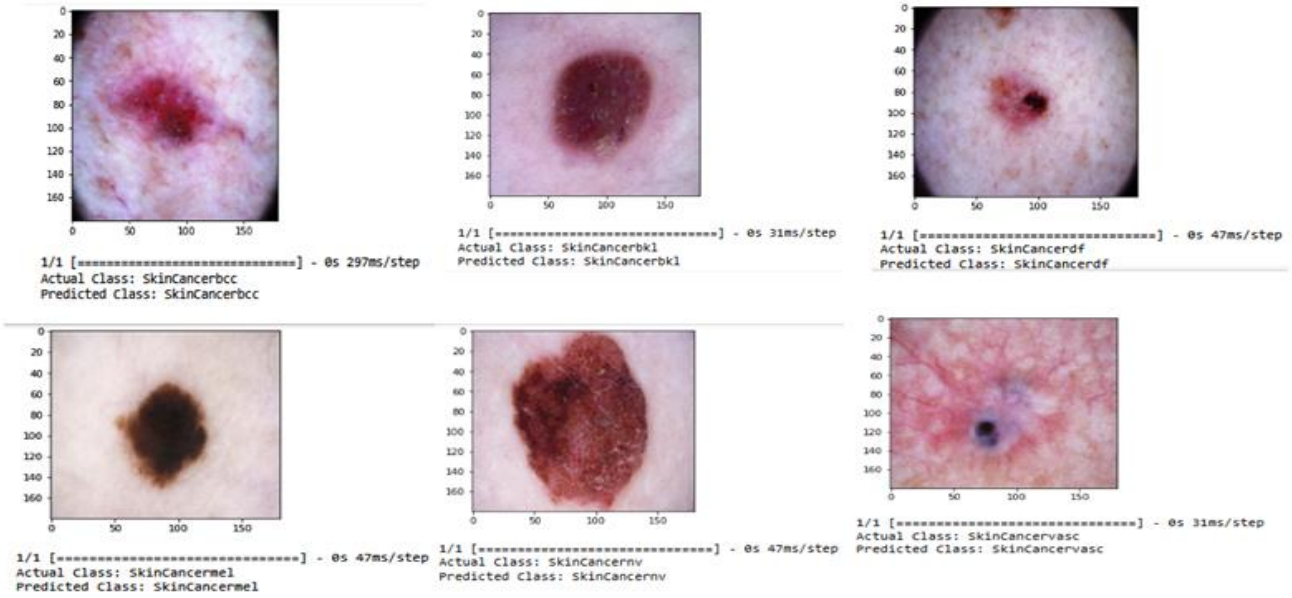

Fig. 6 Comparison between actual and predicted skin cancer classes during model testing.

Figure 6 illustrates how effectively the model can distinguish between classifications such as benign keratosis, basal cell carcinoma, and melanoma and its ability to classify various skin diseases appropriately. It provides a graphic depiction of the model's performance, emphasizing instances where predictions correspond with actual labels and calling attention to any discrepancies or inaccurate classifications. It is crucial to comprehend the model's benefits and drawbacks, particularly in a clinical context where precise diagnosis is crucial. In addition to demonstrating the potential contribution of such technologies to the progress of medical diagnostics, the effective alignment of expected and actual classes represents a significant advancement in using deep learning techniques for skin cancer diagnosis.

5. Conclusion

This research presents DermaNet, a customized Convolutional Neural Network (CNN) for skin cancer classification using the HAM10000 dataset. The influence of dataset imbalance and the impacts of different optimizers and activation functions on classification performance were examined. Our results demonstrate that using oversampling techniques to balance the dataset significantly improves model performance, particularly for minority groups.

After extensive testing, it was determined that the combination of ELU and Nadam generated the best results, with 97.0% accuracy, 92.6% precision, 94.9% recall, and an AUC of 0.98. It is a reliable AI-based diagnostic tool for detecting skin cancer because its design ensures high sensitivity and accuracy. Future studies may use more advanced techniques, such as Generative Adversarial Networks (GANs) for data augmentation, and experiment with different designs to improve classification accuracy. Expanding the dataset to include larger and more diverse samples from other populations may also help to improve the model's generalizability. In summary, this work demonstrates the efficacy of AI-driven methods in medical imaging, particularly in the detection of skin cancer, and it opens up new avenues for investigation into intelligent healthcare systems.

References

[1] Yali Nie et al., "Recent Advances in Diagnosis of Skin Lesions Using Dermoscopic Images Based on Deep Learning," *IEEE Access*, vol. 10, pp. 95716-95747, 2022. [CrossRef] [Google Scholar] [Publisher Link]

[2] Muhammad Qasim Khan et al., "Classification of Melanoma and Nevus in Digital Images for Diagnosis of Skin Cancer," *IEEE Access*, vol. 7, pp. 90132-90144, 2019. [CrossRef] [Google Scholar] [Publisher Link]

[3] Skin Cancer Statistics Melanoma of the Skin is the 19th Most Common Cancer Worldwide, World Cancer Research Fund, 2020. [Online]. Available: https://www.wcrf.org/dietandcancer/cancer-trends/skin-cancer-statistics

[4] G. Alden Holmes et al., "Using Dermoscopy to Identify Melanoma 1200 and Improve Diagnostic Discrimination," *Federal Practitioner*, vol. 35, no. 4, pp. 39-45, 2018. [Google Scholar] [Publisher Link]

[5] Duggani Keerthana et al., "Hybrid Convolutional Neural Networks with SVM Classifier for Classification of Skin Cancer," *Biomedical Engineering Advances*, vol. 5, pp. 1-8, 2023. [CrossRef] [Google Scholar] [Publisher Link]

[6] N. Priyadharshini et al., "A Novel Hybrid Extreme Learning Machine and Teaching–Learning-Based Optimization Algorithm for Skin Cancer Detection," *Healthcare Analytics*, vol. 3, pp. 1-10, 2023. [CrossRef] [Google Scholar] [Publisher Link]

[7] Van-Dung Hoang, Xuan-Thuy Vo, and Kang-Hyun Jo, "Categorical Weighting Domination for Imbalanced Classification with Skin Cancer in Intelligent Healthcare Systems," *IEEE Access*, vol. 11, pp. 105170-105181, 2023. [CrossRef] [Google Scholar] [Publisher Link]

[8] Skin Cancer MNIST: HAM10000, Kaggle. [Online]. Available. https://www.kaggle.com/datasets/kmader/skin-cancer-mnist-ham10000

[9] Stephanie S. Noronha et al., "Deep Learning-Based Dermatological Condition Detection: A Systematic Review with Recent Methods, Datasets, Challenges, and Future Directions," *IEEE Access*, vol. 11, pp. 140348-140381, 2023. [CrossRef] [Google Scholar] [Publisher Link]

[10] C.H. Qiu et al., "Application Review of Artificial Intelligence in Medical Images Aided Diagnosis," *Space Medicine and Medical Engineering*, vol. 34, no. 5 pp. 407-414, 2021. [Google Scholar]

[11] Li Zhang et al., "A Deep Learning Outline Aimed at Prompt Skin Cancer Detection Utilizing Gated Recurrent Unit Networks and Improved Orca Predation Algorithm," *Biomedical Signal Processing and Control*, vol. 90, 2024. [CrossRef] [Google Scholar] [Publisher Link]

[12] Ashwani Kumar et al., "A Novel Skin Cancer Detection Model using Modified Finch Deep CNN Classifier Model," *Scientific Reports*, vol. 14, pp. 1-19, 2024. [CrossRef] [Google Scholar] [Publisher Link]

[13] Krishna Mridha et al., "An Interpretable Skin Cancer Classification Using Optimized Convolutional Neural Network for a Smart Healthcare System," *IEEE Access*, vol. 11, pp. 41003-41018, 2023. [CrossRef] [Google Scholar] [Publisher Link]

[14] H.L. Gururaj et al., "DeepSkin: A Deep Learning Approach for Skin Cancer Classification," *IEEE Access*, vol. 11, pp. 50205-50214, 2023. [CrossRef] [Google Scholar] [Publisher Link]

[15] E. Gomathi et al., "Skin Cancer Detection Using Dual Optimization based Deep Learning Network," *Biomedical Signal Processing and Control*, vol. 84, 2023. [CrossRef] [Google Scholar] [Publisher Link]

[16] S.P. Godlin Jasil, and V. Ulagamuthalvi, "A Hybrid CNN Architecture for Skin Lesion Classification using Deep Learning," *Soft Computing*, 2023. [CrossRef] [Google Scholar] [Publisher Link]

[17] Sachin Gupta et al., "Ensemble Optimization Algorithm for the Prediction of Melanoma Skin Cancer," *Measurement: Sensors*, vol. 29, pp. 1-9, 2023. [CrossRef] [Google Scholar] [Publisher Link]

[18] Yagmur Olmez et al., "Improved PSO with Visit Table and Multiple Direction Search Strategies for Skin Cancer Image Segmentation," *IEEE Access*, vol. 12, pp. 840-867, 2024. [CrossRef] [Google Scholar] [Publisher Link]

[19] Himanshu K. Gajera, Deepak Ranjan Nayak, and Mukesh A. Zaveri, "A Comprehensive Analysis of Dermoscopy Images for Melanoma Detection via Deep CNN Features," *Biomedical Signal Processing and Control*, vol. 73, no. 2, 2023. [CrossRef] [Google Scholar] [Publisher Link]

[20] V. Auxilia Osvin Nancy et al., "Comparative Study and Analysis on Skin Cancer Detection using Machine Learning and Deep Learning Algorithms," *Multimedia Tools and Applications*, vol. 82, pp. 45913-45957, 2023. [CrossRef] [Google Scholar] [Publisher Link]

[21] Dangguo Shao, Lifan Ren, and Lei Ma, "MSF-Net: A Lightweight Multi-Scale Feature Fusion Network for Skin Lesion Segmentation," *Biomedicines*, vol. 11, no. 6, pp. 1-15, 2023. [CrossRef] [Google Scholar] [Publisher Link]

[22] Pavel A. Lyakhov, Ulyana A. Lyakhova, and Diana I. Kalita, "Multimodal Analysis of Unbalanced Dermatological Data for Skin Cancer Recognition," *IEEE Access*, vol. 11, pp. 131487-131507, 2023. [CrossRef] [Google Scholar] [Publisher Link]

[23] Arslan Akram et al., "Segmentation and Classification of Skin Lesions using Hybrid Deep Learning Method in the Internet of Medical Things," *Skin Research and Technology*, vol. 29, no. 11, pp. 1-14, 2023. [CrossRef] [Google Scholar] [Publisher Link]

[24] Maria Tamoor et al., "Skin Lesion Segmentation Using an Ensemble of Different Image Processing Methods," *Diagnostics*, vol. 13, no. 16, pp. 1-14, 2023. [CrossRef] [Google Scholar] [Publisher Link]

[25] Peng Yao et al., "Single Model Deep Learning on Imbalanced Small Datasets for Skin Lesion Classification," *IEEE Transactions on Medical Imaging*, vol. 41, no. 5, pp. 1242-1254, 2022. [CrossRef] [Google Scholar] [Publisher Link]